# ADDIS ABABA UNIVERSITY
# SCHOOL OF GRADUATE STUDIES
# DEPARTMENT OF CHEMISTRY


# Computational Studies of First row Transition metal Complexes of Schiff Base Derived from Ninhydrin and α, L-alanine

BY

Tesfalem G/maraiam

Advisor

Dr. Ahmed Mustefa

Jul, 2009

# ADDIS ABABA UNIVERSITY
# SCHOOL OF GRADUATE STUDIES
# DEPARTMENT OF CHEMISTRY

A Project

Presented to Office of Research and Graduate Programs

Addis Ababa University

Department of Chemistry

In partial fulfillment of the requirements for the Degree of Master of Science in Chemistry

By

Tesfalem G/mariam

Jul, 2009

# ADDIS ABABA UNIVERSITY
# SCHOOL OF GRADUATE STUDIES
# DEPARTMENT OF CHEMISTRY

## Computational Studies of First row Transition metal Complexes of Schiff Base Derived from Ninhydrin and α, L-alanine

TESFALEM G/MARAIM

| **Approved by the Examination Board** | **Signature** |
|---|---|
| Dr. Ahmed Mustefa<br>Advisor | _____ |
| Prof. V.J.T.Raju<br>Examiner | _____ |
| Dr. Mesfin Redi<br>Examiner | _____ |

**DECLARATION**

I, the undersigned declare that this is my original work and has not been submitted for a degree in any other University and all sources of material used for the project have been duly acknowledged.

Name: Tesfalem G/maraim

Signature: _____

This project has been submitted for examination with my approval as University advisor.

Name: Dr. Ahmed Mustefa

Signature: _____

Place and date of submission:

School of Graduate Studies
Addis Ababa University
Jul, 2009

**Acknowledgements**

First of all, I would like to give the greatest possible glory and thanks for my Lord, the son of almighty God. He is the one responsible for the accomplishment of this work in my life according to his eternal plan.

I am deeply indebted to Dr. Ahmed Mustefa for his invaluable guidance, abiding interest, and unreserved support most generously given during the course of my research until its completion and get myself in the core of the stream, computational chemistry. He is the person who devoted his time with me both in the course, seminar and research works of this program. I am also grateful to Dr. Mesfin Redi for his valuable presentation of the course so that I can able to handle this work.

It gives me a great pleasure to express my deep sense of gratitude to my friend Abel Teklemaraim for his moral, material support during this project work, and without his help, this could not be presented, Thanks Abel.

My sincere thanks are also due to my fellow research partners, Meresa Abrha, Teshome Assefa for their cooperation and understanding in any step of the program. I am also thankful to my friends who stood beside me and their continuous encouragement to accomplish the program.

I am also grateful to the department of chemistry at Addis Ababa University and the newly introduced Wolita Soddo University for giving me the opportunity to undertake this postgraduate study and financial support.

Last but not least I want to thank my parents for their love and encouragement throughout the program being sorrow since the death of my lovely sister. Without their constant support I would not be able to present this work.

**Table of Contents** **Pages**

**List of tables** **Pages**

**List of figures** **Pages**

**Acronyms**

| | |
|---|---|
| IR | Infrared |
| UV-Vis | Ultra-Vilotet and Visisble |
| NMR | Nuclear Magnetic Resonance |
| EPR | Electron Paramagnetic Resonance |
| MM2 | Molecular Mechanics of parametric 2 |
| MM3 | Molecular Mechanics of parametric 3 |
| AMBER | Assisted Model Building Energy Refinement |
| OPLS-AA | Optimized Potential for Liquid simulation-All Atoms |
| UFF | Universal Force Fields |
| SD | Slater Determinant |
| HF | Hartree-Fock |
| HF-SCF | Hartree-Fock-Self Consistent Field |
| ZDO | Zero Differential Overlap |
| MNDO | Modified Neglect of Differential Overlap |
| AM1 | Austin Model 3 |
| PM3 | Parametric Model 3 |
| NDDO | Neglect of differential Diatomic Overlap |
| CNDO | Complete Neglect of Differential Overlap |
| INDO | Intermediate Neglect of Differential Overlap |
| DFT | Density Functional Theory |
| LDA | Local Density Approximation |
| GGA | Generalized Gradient Approximation |
| B88 | Becke's 1988 |
| P86 | Perdew 1986 |
| P91 | Perdew 1991 |
| LYP | Lee-Yang-Parr |

| | |
|---|---|
| BLYP | Becke exchange functional –Lee-Yang-Perdew corelation |
| B3LYP | Becke's three parameter exchange Functional with Lee-Yang-Perdew correlation functional |
| B3PW91 | Becke three parameter with Perdew 1991 |
| B1B96 | Becke one parameter of Becke 1996 model |
| PES | Potential Energy Surface |
| ZINDO | Zerner's INDO |

## Abstract

A Density functional theory and semi empirical calculation have been carried out on a first row transition metal complexes, Mn(II), Fe(III), Co(II), Ni(II), Zn(II) to predict molecular properties of the metal complexes chelated to the intermediate Schiff base, IDIPA, derived from ninhydrin and α, L-alanine in their octahedral structure. The hybrid B3LYP method has been used to predict the geometry and IR spectra of the metal complexes. Geometry and infrared spectra of the metal complexes, Mn(II), Fe(II), Co(II), Ni(II), and Zn(II) were calculated with B3LYP method using 6-31G, 3-21G(d), 6-31G(d), 3-21G(d), and 3-21G(d) basis set, respectively, and compared with their experimental data. The electronic spectra of the ligand and metal complexes were also performed with ZINDO method. The geometry of the metal complexes were predicted and the ligand were characterized as tridentate and monobasic potential ligand for the metals in their octahedral structure. The electronic spectral calculation of the metal complexes were clearly indicative of a coordination of six in which the number of ligands, IDIPA, coordinated to the metal vary for the first two metal complexes, Mn(II), Fe(III). The computational prediction of IR spectra and electronic spectra using B3LYP and ZINDO, respectively, are good models reproducing results, which are in good agreement to the experiment.

# 1. Introduction to computational chemistry

The discovery processes of chemistry are more of descriptive and qualitative, but fundamentally it is a quantitative science. The mathematical sciences provide the language for qualitative science and this language is going in many directions as Computational science. [1]
The term theoretical chemistry is therefore defined as the mathematical description of chemistry and computational chemistry is generally used when a mathematical method is sufficiently well developed that it can be automated for implementation on a computer.
Computational chemistry is therefore an outgrowth of theoretical chemistry, which is sought to device and implement quantitative algorithms for organizing massive amounts of data from the laboratory, and for predicting the course and extent of chemical phenomena in situations that are difficult or even impossible to observe directly in the laboratory. [1-4]

Computational chemistry involves a mathematical description of systems of chemical species. The goal is to solve the complex equations such as the Schroedinger equation for electronic and nuclear motion, which accurately describe natural phenomena. In a practical application of computational chemistry, mathematical equations or algorithms are devised to quantitatively describe the physical and chemical phenomena (e.g., energy states, structures, reactivity, positions and momenta of atoms) that occur in a particular system. These algorithms are then programmed in the appropriate computer languages and linked together so that the many millions of calculations required to effectively describe the phenomena can be quickly computed. For example, it might be necessary to evaluate billions of integrals to accurately describe the repulsion of electrons in a complex molecule. The end result is a set of

computational tools that predict the characteristics and behavior of the chemical system.

Computational chemistry can also play an important role in the design of molecules (e.g., new chemical products, materials, catalysts). For example, by reliably predicting thermochemistry (the energy associated with the chemical reaction), it is possible to examine the feasibility of reaction pathways to determine whether a reaction is thermodynamically allowed. Computational chemistry can also be used to reliably predict a wide range of spectroscopic properties (IR, Raman, UV-Vis, NMR, EPR, photo electron) to aid in the identification of chemical species (e.g., reaction intermediates). Electronic structure calculations can also provide useful insights into bonding, orbital energies and shapes, which can be used to target the design of new molecules with selective reactivity. [3]

## 1.1. Molecular mechanics

Molecular mechanics methods are a non-quantum (i.e. classical) mechanical computation for obtaining geometries of gas phase molecules. As a result, molecular mechanics methods are computationally fast. Molecular mechanics methods use empirical force fields to describe the energy of a given configuration. Molecular mechanics calculations are commonly used to predict equilibrium molecular geometries or conformations. Mathematical expressions are used to represent various components of the bonding interactions (bond stretching, bond bending, and torsional interactions). Using these expressions the total energy of a molecule, in a given conformation, is calculated. The energy of a given configuration is calculated as follows.

$$E = E_{bond} + E_{angle} + E_{dihed} + E_{vdw} + E_{ele} \quad \ldots\ldots\ldots\ldots\ldots\ldots\ldots\ldots\ldots\ldots \quad (1.1)$$

Molecular mechanics treats a molecule as an array of atoms governed by a set of classical-mechanical potential functions. The parameters for the potential functions used in the calculation come from experimental data and/or high-level quantum mechanical computations on similar molecules.

The assumption in the technique is that similar bonds in different molecules will have similar properties. This assumption works well so long as the molecules being calculated do not differ significantly from the molecules used to determine the parameters for the force fields. [5]

Molecular mechanics techniques are valuable computations for establishing good starting points of initial geometry for higher-level quantum mechanical computations. The accuracy of the geometries obtained can be as close to the values obtained from higher-order quantum mechanical computations.

There are different molecular mechanics methods (Force field methods) that differ from each other in three main aspects, the functional term of each energy term, the number of cross terms included, and the type information used for fitting the parameters. MM2, MM3, AMBER, OPLS-AA, SYBYL, DRIEDING, UFF etc. [6-7]

## 1.2. Quantum mechanics

Quantum chemistry applies quantum mechanics to problems in chemistry. The postulates and theorems of quantum mechanics form the rigorous foundation for the prediction of observable chemical properties from first principle. The fundamental postulates of quantum mechanics assert that microscopic systems are described by 'Wave functions' that completely characterize all of the physical properties of the system. [1, 4]

Thus Quantum mechanics explicitly represents the electron in a calculation, and so it is possible to derive properties that depend up on the electronic distribution and in particular, to investigate chemical reactions in which bonds are broken and formed. The fundamental postulate of quantum mechanics is that a so called wave function **Ψ**, exists for any (chemical) system, and that appropriate operators (functions) which act up on **Ψ** return the observable properties of the system. In mathematical notation,

$$\vartheta\Psi = e\Psi \quad \text{..... (1.2)}$$

Where, $\vartheta$ –is an operator

$e$ - is a scalar value for some properties of the system

When the above equation holds, Ψ is called an eigen function and $e$ an eigen value, by analogy to matrix algebra Ψ to be an $N$ –element column vector, $\vartheta$ - to be an $N$ x $N$ square matrix and $e$ to remain scalar quantity. When the operator in the above equation returns the system energy $E$ as an eigen value, is called the Hamiltonian operator. Thus,

$$\hat{H}\Psi = E\Psi \quad \text{..... (1.3)}$$

(which is the time independent Schrödinger equation)

The Hamiltonian is composed of the kinetic and potential energy of the electron and nucleus, which can be described as operators.

$$\hat{H} = \hat{T} + \hat{V} \quad \text{..... (1.4)}$$

Casting the Hamiltonian into mathematical notation,

$$H = -\sum_{i=1}^{N} \frac{\hbar^2}{2M_e}\nabla_i^2 - \sum_{A=1}^{M} \frac{\hbar^2}{2M_A}\nabla_A^2 - \sum_{i=1}^{N}\sum_{A=1}^{M} \frac{e^2 Z_A}{r_{iA}} + \sum_{i=1}^{N}\sum_{j>i}^{N} \frac{e^2}{r_{ij}} + \sum_{A=1}^{M}\sum_{B>A}^{M} \frac{e^2 Z_A Z_B}{R_{AB}} \quad \text{..... (1.5)}$$

where, $i$ and $j$ run over $N$ electrons, $A$ and $B$ run over $M$ nuclei, $\hbar$- is Planck's constant, $\nabla^2$ - is Laplacian operator, $Z_A$ and $Z_B$ atomic numbers of nucleus A and B respectively, e- is the charge on the electron, $r_{ij}$ and $R_{AB}$ are the interelectron and internuclei distances, respectively.

This is by far the basic in all quantum mechanical calculation for chemical properties.

The Hamiltonian (Eq.1.3) contains pair wise attraction and repulsion terms, imply that no particle is moving independently of all of the others (the term 'correlation' is used describe this interdependency). Thus, in order to simplify the problem, quantum chemical calculations invoke a so-called Born-Oppenhiemer Approximation. It simplifies the general molecular problem by separating nuclear and electronic motions, which allow the two parts of the problem, solved independently, i.e. the total Hamiltonian (Eq. 1.3) is separated into electronic and nuclear Hamiltonians. This separation is based on the fact that the mass of a typical nucleus is much heavier than that of electrons so that the nucleus moves very slowly than electrons.

$$\hat{H}_{ele} = -\sum_{i=1}^{N} \frac{\hbar^2}{2M_e} \nabla_i^2 - \sum_{A=1}^{M} \frac{\hbar^2}{2M_A} \nabla_A^2 - \sum_{i=1}^{N} \sum_{A=1}^{M} \frac{e^2 Z_A}{r_{iA}} \quad \text{..... (1.6)}$$

Therefore, all quantum mechanical calculations are based on this principle and hence are called Electronic Structure Methods. Electronic structure methods are therefore the use of laws of quantum mechanics rather than classical physics as the basis for their computations. [3-5]

For any but the smallest systems, however, exact solutions to the Schrödinger equation are not computationally practical. Electronic structure methods are characterized by their various mathematical approximations to its solution. Some of the basis electronic structure methods are reviewed below.

### 1.2.1. Hartree – Fock method

An accurate solution of the Schrödinger equation is only possible when the system contains only one or two electrons. For molecules containing multi-electrons, the best approach of finding a good wave function lies in first calculating an approximate wave function using the Hartree-Fock procedure. This method is the basis for the use of atomic and molecular orbitals in many electron systems. [2]

The Hamiltonian for many electron systems is now separable into a one electron Hamiltonian in which only the one electron kinetic energy and nuclear attraction terms are to be expressed as,

$$\hat{H} = \sum_{i=1}^{N} \hat{h}_i \quad \text{..... (1.7)}$$

Where $N$ is the total number of electrons and $h_i$ is the one electron Hamiltonian defined by

$$\hat{h}_i = -\frac{1}{2}\nabla_i^2 - \sum_{k=1}^{M} \frac{Z_K}{r_{ik}}$$

Because the Hamiltonian operator defined by the above equation is separable, its many electrons eigen functions can be constructed as product of one electron eigen functions. That is,

$$\Psi_{HP} = \Phi_1 \Phi_2 \Phi_3 \Phi_4 \ldots \Phi_N = \prod_i^N \Phi_i \quad \text{..... (1.8)}$$

(The Hartree product wave function)

The Hartree product wave function is slightly modified in order to characterize the relativistic and antisymmetric nature of the electrons and satisfy the constraints. [1, 4]

The total electronic wave equation must be antisymmetric with respect to the interchange of any two-electron coordinates. Hence, the antisymmetry nature of the wave function can be achieved by building it from Slater Determinants (SDs). The columns in a Slater Determinant

are single electron wave functions, orbitals, while the electron coordinates are along the rows. The one-electron functions are thus molecular orbitals (MO), which are given as a product of a spatial orbital times a spin function (α or β) also known as spin orbitals and may be taken orthonormal.

For the general case of *N* electrons and *N* spin orbitals, a Slater Determinant is given as

$$\Psi(1,2,\ldots,N)=\frac{1}{\sqrt{N!}}\begin{vmatrix}\Phi_1(1) & \Phi_2(1) & \Phi_3(1)\ldots & \Phi_N(1)\\ \Phi_1(2) & \Phi_2(2) & \Phi_3(2)\ldots & \Phi_N(2)\\ \Phi_1(3) & \Phi_2(3) & \Phi_3(3)\ldots & \Phi_N(3)\\ \vdots & \vdots & \vdots & \ddots\\ \Phi_1(N) & \Phi_2(N) & \Phi_3(N)\ldots & \Phi_N(N)\end{vmatrix} \quad \ldots\ldots\ldots\ldots\ldots\ldots \quad (1.9)$$

where $\Phi_i$ is a spin orbital, i.e. a product of spatial orbital and an electron spin eigen function and $1/\sqrt{N!}$ is the normalization factor. Solving the Schröedinger equation for an atom with N electrons is a formidable computational task because of the numerous electron-electron repulsion terms, $1/r_{ij}$. In order to calculate the electron repulsion of one electron, the wavefunctions for the other electrons must be known and vice versa. This procedure is called self-consistent field (SCF).

The Hartree-Fock self-consistent field (HF-SCF) approach assumes that any one electron moves in a potential that is a spherical average due to the other electrons and the nucleus.

The spherically averaged potential for an electron is expressed as a single charge that is centered on the nucleus and varies with the position r in the potentially averaged sphere. The Schröedinger equation is then numerically solved for that electron in the spherically averaged potential. The HF model is a kind of starting point, either additional approximation may be invoked leading to semiempirical methods, or it can be improved by adding additional determinants, generating solutions, which can be

made to converge toward the exact solution of the electronic Schröedinger equation.

### 1.2.2. Semiempirical methods

Semiempirical methods represent a “middle road” between the mostly qualitative results available from molecular mechanics and the computationally time-consuming quantitative results available from *Ab initio* methods. Semi-empirical methods are a good choice for many users, especially those new to molecular modeling that are less interested in research-quality numerical results, and are more interested in developing their ability to use computing to understand structure, properties, and activities.

These methods address the issue of limitations on calculations of large molecules and the length of computing time needed with *Ab initio* methods. It does so by making several large assumptions, including ignoring core (non-valence) electrons and making major simplifications of the mathematics. Semiempirical methods use many of the same mathematics as are found in the Hartree-Fock method, but look to reduce the computing time by replacing some of the mathematics with data (known as parameters) derived from experimental and computed data. Semiempirical methods use a type of approximation known as zero differential overlap, or ZDO. These methods parameterize some of the calculations. Specifically, semiempirical methods will replace the calculation of the two-electron integrals with data from spectroscopic experimental data. The various types of semi-empirical methods all use different numbers and types of parameters, which affect the quality of the calculation. The term semi-empirical comes from the fact that some of the calculations come from empirical data. Modern semi-empirical methods include MNDO, AM1, and PM3 are all based on the Neglect of

Differential Diatomic Overlap (NDDO) integral approximation, while older methods use simpler integral schemes such as CNDO and INDO. All three approaches belong to the class of Zero Differential Overlap (ZDO) methods, in which all two-electron integrals involving two-center charge distributions are neglected. A number of additional approximations are made to speed up calculations (see below) and a number of parameterized corrections are made in order to correct for the approximate quantum mechanical model. How the parameterization is performed characterizes the particular semiempirical method. For MNDO, AM1, and PM3 the parameterization is performed such that the calculated energies are expressed as heats of formations instead of total energies. [4]

### *1.2.3. Ab initio* methods

The term "*Ab initio"* comes from Latin meaning from 'the beginning'. The implication is that the computations are exact with no approximations. This is certainly not the case, as the Schroedinger equation for more than a two-body system cannot be solved without approximations and using approximation techniques. What "*Ab initio"* does mean in this context is that the integrals involved in the Schröedinger equation for the system are explicitly solved without the use of empirical parameters. These methods are unarguably the most accurate, as well as the most difficult, of all of the techniques currently in use in the field of molecular modeling. As its name indicates, the *Ab* initio methods really does start 'from the scratch, beginning with just the molecular structure and a few constants; the speed of light (c), Plank's constant (h), the mass ($m_e$) and charge ($q_e$) of the electron.

*Ab initio* electronic structure methods have the advantage that they can be made to converge to the exact solution, when all approximations are sufficiently small in magnitude.

*Ab initio* methods starts calculation from HF formalism where HF theory makes the fundamental approximation that each electron moves in the static electric field by all of the other electrons and then proceeds to optimize orbitals for all of the electron in a self consistent fashion subject to a variational constant. Hence, calculations give higher electronic energy than the exact calculation. The chief error in the HF approximation derives from ignoring the correlated motion of each electron with each other. [4, 8]
In post HF calculation, the wave function is constructed to include electron correlation and accurately describe the molecular orbitals. Therefore, an *Ab initio* SCF-MO calculation uses the approximation of taking Ψ as an antisymmetrized product of one electron spin orbitals and uses a finite (and hence in complete) basis set. *Ab initio* methods differ in their accuracy and level of theory how the electron correlation is treated. [1, 4, 7]

There are many available *Ab initio* methods for calculating electron correlation; Configuration Interaction (CI), Many Body Perturbation, the Møller Plesset ($MP_n$), and Coupled Cluster (CC).

A configuration interaction wave function is a multiple-determinant wave function constructed by starting with the HF wave function and making new determinants by promoting electrons from the occupied to unoccupied orbital. Configuration interaction calculations can be very accurate, but the cost in CPU time is very high.

In contrast to the HF method, in order to account for electron correlation CI uses a variational wave function that is a linear combination of configuration state function (CSFs) built from spin orbitals.

The full CI method forms the wave function $\Psi$ as a linear combination of the HF determinant and all possible determinant.

$$\Psi_{CI} = \sum_{I=0} C_I \Phi_I \quad \text{..... (1.10)}$$

$$\Psi_{CI} = C_0 \Psi_0 + C_I \Phi_1 + \cdots$$

where $\Psi$ is usually the electronic ground state of the system, and the 0-indexed term is the Hartree-Fock level. [3, 4]

The number of excitations used to make each determinant classifies configuration interaction calculations. If only one electron has been moved for each determinant, it is called a configuration interaction single-excitation (CIS) calculation. CIS calculations give an approximation to the excited states of the molecule, but do not change the ground-state energy. Single-and double excitation (CISD) calculations yield a ground-state energy that has been corrected for correlation. Triple-excitation (CISDT) and quadruple-excitation (CISDTQ) calculations are done only when very-high-accuracy results are desired. Due to the long CPU time and immense hardware required for CI calculation, the method is limited to relatively small systems. [2]

Coupled cluster calculations are similar to configuration interaction calculations in that the wave function is a linear combination of many determinants. However, the means for choosing the determinants in a coupled cluster calculation is more complex than the choice of determinants in a CI. Like CI, there are various orders of the CC expansion, called CCSD, CCSDT, and so on. A calculation denoted CCSD(T) is one in which the triple excitations are included perturbatively rather than exactly. The advantage of doing coupled cluster calculations is that it is a size extensive method. Often, coupled-cluster results are a

bit more accurate than the equivalent size configuration interaction calculation results. When all possible configurations are included, a full coupled-cluster calculation is equivalent to a full CI calculation. [1-2, 9]

Correlation can be added as a perturbation from the Hartree-Fock wave function. This is called Møller-Plesset perturbation theory. Perturbation theory is based up on dividing the Hamiltonian in to two parts;

$$H = H_0 + \lambda^{(1)} H^{(1)} \quad \text{..... (1.11)}$$

Such that $H_0$ is the unperturbed Hamiltonian and $\lambda H$ is a perturbation applied to $H_0$.

In mapping the HF wave function onto a perturbation theory formulation, HF becomes a first-order perturbation. Thus, a minimal amount of correlation is added by using the second order MP2 method. Third-order (MP3) and fourth-order (MP4) calculations are also common. The accuracy of an MP4 calculation is roughly equivalent to the accuracy of a CISD calculation. MP5 and higher calculations are seldom done due to the high computational cost. [2, 10-11]

The *Ab initio* methods calculation is therefore greatly affected by size of the basis set, i.e. the number of electrons. Hence, the electron correlation becomes more practical and challenging if the size of the molecules becomes larger and larger. The applications of Ab initio methods are thus limited to small size molecules and cost of the application is greatly increased for larger molecule calculation.

### 1.2.4. Density Functional Methods

Calculations based on wave function are difficult because the wave function depends on spin and three spatial coordinates for every electron, i.e. $4N$ for $N$ electrons. Hence, the complexity of wave function increases with number of electrons. [4]

The dependence on total number of electrons immediately suggests that a useful physical observable would be the electron density $\rho$, since integrated over all space gives the total no of electrons, $N$, i.e.

$$N = \int \rho(r)dr \quad \text{..... (1.12)}$$

Therefore, the electron density is dependent only on three coordinates, which is not greatly affected by system size.

The basis for the density functional theory is thus the electro density that was first proved by Hohenberg and kohn in which the ground sate electronic energy is determined completely by the electron density, $\rho$. [12-13]

The total energy can be stated as;

$$E_{DFT}[\rho] = T[\rho] + E_{ne}[\rho] + E_{ee}[\rho] \quad \text{..... (1.13)}$$

The energy related to the electro-electron ($E_{ee}[\rho]$) interaction is therefore expressed as result of two terms, i.e., the electron-electron coulombic energy, $J[\rho]$ and the electron-electron exchange energy $K[\rho]$. Thus the above equation can be rewritten as,

$$E_{DFT}[\rho] = T[\rho] + E_{ne}[\rho] + J[\rho] + K[\rho] \quad \text{..... (1.14)}$$

The last term in Eq.1.14 is not accurately known and includes the exchange correlation functional. The definition of exchange and correlation in DFT, are thus local that only depends on the density at a

given point and in the immediate vicinity (via derivative of the density) or non-local in which the electron density has also gradients. The major problem in DFT is therefore expressing the exchange correlation in a more accurate as well as suitable formulas. [1]

Hence, the difference between DFT methods is the choice of the functional form of the exchange-correlation energy. The difference of exchange-correlation energy with respect the electron density leads to different approximation methods. The first approximation was simply that electron density $\rho$ varies extremely slowly with position and the resulting and the resulting $E_{XC}[\rho]$ is given by,

$$E_{XC}^{LDA}[\rho] = \int \rho(r)\varepsilon_{XC}(\rho)dr \quad \text{..... (1.15)}$$

Where $\varepsilon_{XC}(\rho)$ is the exchange plus correlation energy per electron in a homogenous electron gas with electron density $\rho$, this equation is therefore the Local Density Functional Approximation (LDA). [7, 14]

A lot of improvements over the correlation functional is done that the correlation functional is not dependent only on the local value of the density, but on the extent to which the density is locally changing, i.e., the gradient of the density also called generalized gradient approximation (GGA). The first widely introduced GGA exchange functional was by Becke (abbreviated as B) in which the functional adopts a mathematical form that has correct asymptotic behavior at long range for the energy density. With respect to the correlation functional, corrections to the correlation energy density include, B88, P86, P91, and LYP. [15-17]

Any exchange functional can therefore be combined with any correlation functional. For example, the notation BLYP denotes a Density Functional calculation done with Becke 1988 exchange functional and the Lee-Yang-

Parr correctional functional. The foundation for the use of DFT methods in computational chemistry was the introduction of orbitals by Kohn-Sham.

In an attempt to improve the accuracy of the exchange energy, Becke mixed HF exchange with pure local density exchange and empirically fitted the resulting hybrid exchange functional to give the best agreement with experimental values. Example, B3LYP, B3PW91, and B1B96 are commonly used hybrid DFTs. Currently, the most popular method B3LYP (where the 3 indicates three parameters functional) functional is an absolute shooting star and soon developed into by far, the most popular and most widely used functional including in such difficult areas as open shell transition metal chemistry. Therefore, with a few exceptions, DFT is the most cost effective method to achieve a given level of quantitative accuracy. It includes electron correlation with less computational expense. It is typically the method used to calculate transition metal complexes. In DFT, the total energy is expressed in terms of the total one-electron density rather than the wave function. [18-19]

## 1.3. Basis set in computational chemistry

A basis set in chemistry is a set of functions used to create the molecular orbitals, which are expanded as a linear combination of such functions with the weights or coefficients to be determined. Usually these atoms are atomic orbitals, in that they are centered in the two atoms. Atom centered basis set sets are comprised of atomic functions representing the electron population at a given distance from the nucleus and can be thought of as being atomic orbitals. There are number of different types of atom centered basis functions available, Slater Type Orbitals (STO) which are the form:

$$R(r) = Nr^{n} e^{-\zeta r} \quad \text{..... (1.16)}$$

Where $n$ is the principal quantum number, $N$ is normalization constant, $r$ is the distance from the nucleus and $\zeta$ (*zeta*) is a constant related to the atomic charge of the nucleus. Unfortunately, STOs are often impractical for quantum chemical calculations as some of the integrals are difficult or even impossible.

By far the most popular type of basis sets used in quantum chemistry are those based on Gaussian functions, Gaussian Type orbitals (GTOs), these have the form:

$$R(r) = x^{a} y^{b} z^{c} e^{-\alpha r^{2}} \quad \text{..... (1.17)}$$

A determines the spread of the function, r is the distance from the nucleus, *x, y, z* are cartesian variables and *a, b, c* determine the order of the function. The advantage of the Gaussian function is that less computer time is required to evaluate the integrals. [1, 4]

Minimal basis sets contain the minimum number of basis functions that are needed to describe for each atom. However, form computational chemists' point of view, minimal basis sets are often not good enough for quantum calculation. Thus, the basis set can be expanded in a number of ways to best represent the atomic orbitals. These minimal basis sat can be named as STO-nG, represents that *n* primitive Guassian functions for each STO orbitals. Examples of commonly used minimal basis sets are STO-2G, STO-3G, STO-6G.

A Split Valence basis set is an alternative approach, which is highly popular, is to split only the basis sets used for valence electrons, the rational being that the chemical properties of interest are affected by the valence rather than the core electrons. The inner-shell atomic orbitals are represented by one basis function and the valence orbitals are represented by two or more basis functions. The number of functions

assigned to valence orbitals characterizes Split valence basis sets. Double zeta basis sets use two basis functions to describe valence electrons, and triple zeta use three functions, and so forth. The number of Gaussian functions used to describe inner and outer shell electrons denotes basis sets developed by Pople and coworkers. Commonly used split valence basis sets include, 3-21G, 4-31G, 6-31G, 6-311G. The general notation for split valence can be represented as *K-nlmG,* where K is the number of primitive core function, *nl*-number of contracted valence function and *m* is the number of primitive function in 3rd contraction. To increase the quality of the basis set polarization and diffuse functions are added to account the chemical bonding and outer most weakly bond electrons. Examples, 6-31G(d), and 6-311G(d, p).

Models of a chemical system generally consist of the combination of a theoretical method such as HF and B3LYP with a basis set. Each such unique pairing of method with basis set represents a different approximation to the Schrödinger equation. Hence, choosing a model of a chemical system, almost always involves a trade-off between accuracy and computational cost. More accurate methods and larger basis sets make jobs run longer. Larger basis sets approximate more accurately the orbitals by imposing fewer restrictions on the locations of the electrons in space. Such calculations are also more expensive because they require computing more integrals. [20, 21]

## 2. Molecular properties

In any computational quantum chemistry calculation, the physical observable calculated from the electronic calculation should physically meaningful.

Computational chemistry can be used to describe a diversity of chemical systems with a wide range of complexity. At the quantum molecular level, chemical systems of hundreds of atoms can be modeled today, and highly accurate calculations are possible for up to 10 atoms. More approximate classical atomistic methods can handle systems up to millions of atoms, depending on the time scale. There are many potential applications of computational chemistry in chemical processes where predicting the characteristics and behavior of a system may be beneficial. By predicting a system's behavior, computational chemistry can potentially be used to improve the efficiency of existing operating systems as well as the design of new systems. It can help to shorten product and process development cycles, optimize processes to improve energy efficiency and environmental performance, and solve problems as they arise in plant operations.

Computational chemistry can also assist in the design and optimization of new and existing processes and products. It can be used to reduce the costs of development, improve energy efficiency and environmental performance, and increase productivity and profitability. Although computational chemistry is currently being applied in the chemical industry to some degree, it is difficult, costly, and could see much greater use. There are significant limits to the type and size of problems that can be modeled, as well as the validation and reliability of the results. [2, 4]

Therefore, it is possible to predict different molecular properties that can easily characterize the molecule under study from quantum chemical

calculation. A lot of molecular properties can easily determined using appropriate quantum chemical methods, geometrical structures, electronic energy levels (UV and Visible spectra), thermochemistry ($\Delta H$, $\Delta S$, $\Delta G$, $C_V$, $C_P$) primarily gas phase, potential energy surface (barrier heights, transition states) with a treatment of dynamics that leads to reaction rates and mechanisms, ionization potentials, electron affinities, Frank-Condon factors (transition probabilities, vibronic intensities), IR and Raman intensities, dipole moments, polarizabilities, electron density maps and population analyses as well as magnetic shielding tensors-NMR spectra. [22-24]

## 2.1. Geometry Optimization

To calculate the properties of a molecule, a well-defined structure should be at foremost generated. Thus the process of finding the arrangement of nuclei for which the potential energy is a minimum is known as geometry optimization. The geometry optimization procedure involves making an initial guess for the geometry and then calculating the derivative (gradient) of the potential energy with respect to each of the nuclear coordinates. At a stationary point (lowest values on a potential energy surface);

$$g = \frac{\partial E}{\partial R_i} = 0 \quad \text{and} \qquad \frac{\partial^2 E}{\partial R_i^{\,2}} > 0 \text{ for all } i$$

the gradient represents the force acting upon each atom. These energy gradients are then used to obtain a new geometry that is likely to be closer to the equilibrium geometry. This process is repeated until the energy gradients (forces) approach zero, indicating that equilibrium geometry has been found. Geometry-optimization of molecular structures is a fairly routine task; in that efficient and reliable optimization methods

exist for the most common electronic-structure methods. The first step in any quantum chemical calculation is to find the optimized structure. [4]

## 2.2. Molecular vibrational frequencies

The vibrational states of a molecule are observed experimentally via infrared and Raman spectroscopy. These techniques can help to determine molecular structure and environment. In order to gain such useful information, it is necessary to determine what vibrational motion corresponds to each peak in the spectrum. This assignment can be quite difficult due to the large number of closely spaced peaks possible even in fairly simple molecules. In order to aid in this assignment, many workers use computer simulations to calculate the vibrational frequencies of molecules.

Every computational chemistry program defaults to predicting the harmonic vibrational frequencies, which are the frequencies determined from the second-derivative of the potential energy surface according to the harmonic oscillator approximation:

$$\frac{\Delta E_{\upsilon}}{hc} = \bar{\nu}_i = \frac{1}{2\pi C}\sqrt{\frac{\kappa_i}{\mu}} \quad \text{..... (1.18)}$$

Where $\bar{\nu}$ is the fundamental vibrational frequency, $\kappa$ is the force constant $\mu$ -reduced mass of the corresponding atoms.

Not all molecular vibrations lead to observable infrared absorption. In general, a vibration must cause a change in the change distribution with in a molecule to absorb infrared light. Hence, a vibrational transition is said to be IR active, if the dipole moment of the molecule changes during vibration.

$$\left(\frac{\partial \mu_g}{\partial q_i}\right) \quad \text{..... (1.19)}$$

The greater the change in charge distribution, the stronger the absorption, and intensities of vibrational bands in IR spectra depend on the square of derivatives of the dipole moment with respect to the normal modes.

$$I_{IR} \propto \left|\frac{\partial \mu}{\partial q}\right|^2 \quad \text{..... (1.20)}$$

In order to predict the stretching frequency with in the harmonic oscillator equation all that is needed is the 2nd derivatives of the energy with respect to bond stretching computed at the equilibrium geometry, i.e., $\kappa$. The importance of $\kappa$ has led to considerable effect to derive analytical expression for second derivatives and they are now available in most Ab-initio methods and DFT methods. Harmonic vibrational frequencies obtained from computational methods are always larger than the experimental ones (10%). The major source of this disagreement is the neglect of anharmonicity effects in the theoretical treatment, the potential energy surface is of course not exactly harmonic, and the true vibrational frequencies will have contributions from third, fourth, and higher derivatives of the potential energy surface. Thus, theoretical harmonic frequencies are almost always too high compared to experimentally measure fundamental frequencies. Errors also arise because of the incomplete incorporation of electron correlation and the use of finite basis sets. Pretty good estimates of experimental fundamental frequencies can be obtained by multiplying the harmonic frequencies calculated at a given quantum chemical method by an empirically found scale factor. HF calculation of fundamental vibrational frequencies over emphasizes bonding, so all force constants are too large, and thus so are all frequencies. The pure DFT functional BLYP requires essentially no scaling i.e., its errors are random about the experimental values while the hybrid functionals require scale factors consistent with their inclusion of some HF character. However, application of a constant

scaling factor for the fundamental frequencies calculated at different theory level and basis set improves their accuracy enormously. [1, 4, 25-26]

A vibrational frequency calculation must be preceded by a geometry optimization using the same method and basis set as used for the frequency calculation. Frequencies calculated at a point that is not a stationary point are not true vibrational frequencies.
Different motions of a molecule will have different frequencies. As a general rule of thumb, bond stretches are the highest energy vibrations. Bond bends are somewhat lower energy vibrations and torsional motions are even lower. The lowest frequencies are usually torsions between substantial pieces of large molecules and breathing modes in very large molecules.

## 2.3. UV-Visible Spectral Calculation

The photon energy in the UV-visible range (200-700 nm) is sufficient to promote or excite a molecular electron to a higher energy orbital. Consequently, absorption spectroscopies carried out in this region are called Electronic Spectroscopy. Thus, electronic excited states are most relevant when considering absorption spectroscopy.

As a rule, energetically favored electron promotion will be from the highest occupied molecular orbital (HOMO) to the lowest unoccupied molecular orbital, and the resulting species is called an excited state. Thus, when sample molecules are exposed to light having an energy that matches a possible electronic transition within the molecule, some of the light energy will be absorbed as the electron is promoted to higher energy orbital. For any purpose, transition of lowest energy is the most

important. For most molecules, the lowest energy occupied molecular orbitals are the σ orbitals, which correspond to σ bonds. The π orbitals lie at higher energy levels, and the orbitals that hold unshared pairs, the nonbonding (n) orbitals, lie at even higher energies. The unoccupied, or antibonding orbitals, (π*, σ*), are the orbitals of higher energy.

Not all of transitions are observed. Certain transition, called selection rules, must be considered. [27]

It is shown that the probability of a transition between two states will be induced by the oscillating electric field of light wave is proportional to the square of the transition moment. For an electronic transition, the transition moment integral has the form,

$$\mu_{fi} = \int \psi_f^{*} \hat{\mu} \psi_i d\tau \quad \text{..... (1.21)}$$

Where the star denotes an excited state and $\hat{\mu}$ is the transition dipole moment operator and the *fi* are the final and initial states of the transition.

Therefore a transition is allowed if the transition dipole from the above is different from zero. But if transitions are forbidden, it does not mean that no transition at all, but the transition are not allowed by the selection rules. The two selection rules are Orbital symmetry and spin multiplicity. Hence, a transition is allowed by orbital symmetry if the initial and final states when multiplied by the dipole moment operator results in total symmetry (identity symmetry).

The spin multiplicity selection rule suggests that there should be no change in spin multiplicity, i.e. ΔS=0. Therefore, when a transition is spin and symmetry allowed, very intense transitions are observed. Forbidden transitions show weaker intensities, as they are not allowed by any of the selection rules. A first insight of the intensity is also derived from the oscillator strength (*f*), which is dimensionless quantity such that the allowed transitions are nearly one. [28-29]

One of the principal techniques currently used for studying transition metal complexes is thus the electronic absorption spectroscopy. The electronic absorption spectrum often provides quick and reliable information about the arrangement of ligands around the metal ion. Studying the electronic spectra can provide details about the structure and bonding in complexes. For example, octahedral complexes are readily distinguished from the tetrahedral ones on the basis of the position and intensity of their absorption bands. The number of bands, their frequency and molar absorptivities should all be considered. It is necessary to compare the solution spectrum with that of the solid sate to be sure that the structure of the complex remains the same in solution as well as in the solid state. In solution, the changes may involve ligand replacement by the solvent, ligand rearrangement or increase in the coordination number by solvation. The electronic transitions of metal complexes having organic ligands are classified into three classes.

- Metal-localized *d-d* transitions
- Ligand-localized $\pi \rightarrow \pi^*$ transitions
- Metal to ligand charge transfer $d \rightarrow \pi^*$ (MLCT)

The usually allowed electronic transitions for the metal complexes are the intraligand transitions, i.e. the transitions with in the ligand molecules and metal to ligand or ligand to metal electron transfer transitions. For the transition metals of the 3d series, the intraligand and charge transfer bands are generally at higher energies than the ligand field (d-d) transitions. The electronic absorption transition bands of metal complexes resulting from the d-d transitions are often referred to as ligand field or crystal field bands because their energies shift with positions of the ligand in the spectrochemical series. If the intense bands arising from the allowed transitions extend in to the visible region they may overlap with one or more of the bands due to d-d transitions. Hence, one of the characteristic features of many d-block metal complexes is

therefore their color. The colors are due to absorption of light in the visible region of the spectrum. Absorption bands in electronic spectra for d-block complexes are generally broad since transitions involving d-d transition are generally forbidden. A lot of quantum chemical methods are available now a days providing theoretical calculation of the possible excitations. Most commonly used are of Ab initio methods, configuration interaction (CI), and the time dependent DFT, TD-DFT methods as well as the semiempirical ZNIDO method. [30]

## 3. Transition Metal Complexes

Compounds of the transition elements account for the majority of colored inorganic materials, and many pigments are relatively simple derivatives of these elements; however, not all transition-element compounds are colored. The elements occur at the transition point in the periodic table where the *d* orbitals are being filled. The first row transition elements coincide with the filling of the 3*d,* the second row with the filling of the 4*d,* and the third row with the filling of the 5*d* orbitals. The transition elements are possessing filled or partially filled valence *d* orbitals in one or more of its oxidation states. One of the consequences the open (incompletely filled) $d^n$ configuration of transition-metal ions may be the presence of one or more unpaired electrons. Such compounds could be described as paramagnetic metals.

From the outer configurations of the transition metals and detailed spectroscopic investigations confirm that the 3*d* orbitals lay at higher energies than the 4s orbitals.

Many of the compounds formed by transition metals are of a complex constitution, and they are accordingly known as complexes. The term complex is used to describe a coordination compound in which the acceptor is a metal (usually, but not necessarily, a transition metal) atom

or ion and the donor is called the ligand. Ligands, which interact with a metal ion through two or more donor atoms, are of particular importance in coordination chemistry. [31-33]

The number of potential metal binding sites in a ligand is therefore indicated by use of terms monodentate, bidentate, tridentate, etc. Polydentate ligands, which are flexible enough so that two or more of their donor atoms can wrap around and bind to same metal are called chelating ligands.

A Schiff base (or azomethine) is a potential metal binding function due to σ, π–interacting capability towards metal ions that can act as a tridentate ligand forming two stable five membered rings on complexation. Schiff bases are formed when the amino acid is (α, L-alanine) made to react with ninhydrin and proceed to give Schiff base upon passing many intermediates. They are good ligands for metal ions. Ketimine is therefore the first intermediate before the reaction goes to completion to produce a Schiff base. It is this intermediate of the potential ligand to metal ions, acting as a tridentate ligand forming a complex. The Schiff base formed from ninhydrin and α, L-alanine has the intermediate, which is the potential ligand for the transition metal complexes.

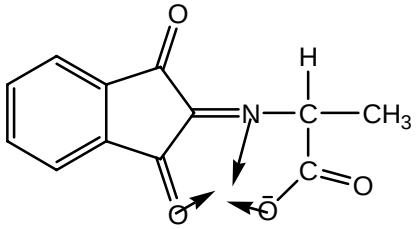


Ketimine intermediate

**Fig**.**I** Possible metal binding centers of a Schiff base derived from ninhydrin and an α, L-alanine

In the presence of metal ions, the reaction between the ninhydrin and amino acids do not proceed to the final step, stops at the first step, i.e, forming a highly colored complex with the Schiff base. The formation of

this stable complex has very prime importance in biological and physiological characteristics of the amino acid. [34-35]

The ligand, which is monobasic and tridentate is extensively form a stable complex so that the formation of Ruhemman's purple is stopped at the intermediate state. The formation of this stable complex provides a wide application and possesses chemical and spectroscopic characteristics, which need further investigation and has very prime importance in biological and physiological characteristics of the amino acid. Experimentally, the complex is synthesized from different 3d transition metal salts and a characteristic colors are observed. Characterization of these metal complexes leads to further application and synthesis of such kind of complexes from different amino acids.
The electronic structure of the *d* metal complexes can be greatly affected by the ligand. In the crystal field theory, a ligand lone pair is modeled as a point negative charge that repels electrons in the *d* orbitals of the central metal ion and the resulting splitting of the *d* orbitals into groups of different energies. It is simply the overlap of d-orbitals with ligand orbitals to form molecular orbitals.

## 3.1. Computational aspects of transition metal complex

There is a growing interest in modeling transition metals because of its applicability to catalysts, bioinorganics, materials science, and traditional inorganic chemistry. Unfortunately, transition metals tend to be extremely difficult to model. This is so because of a number of effects, which are important to correctly describing these compounds. The problem is compounded by the fact that the majority of computational methods have been created, tested, and optimized for organic molecules.

Some of the techniques that work well for organics perform poorly for more technically difficult transition metal systems.

Nearly every technical difficulty known is routinely encountered in transition metal calculations. Calculations on open-shell compounds encounter problems due to spin contamination and experience more problems with SCF convergence. For the heavier transition metals, relativistic effects are significant. Many transition metal compounds require correlation even to obtain results that are qualitatively correct. Compounds with low-lying excited states are difficult to converge and require additional work to ensure that the desired states are being computed. Metals also present additional problems in parameterizing semiempirical and molecular mechanics methods. [2]

More over, the fractional occupation of the *d* shells frequently gives rise to manifold of close lying electronic states, each with different chemical behavior. The near degeneracy problem for transition metal systems is furthermore enhanced by the fact that *d* bonds are often formed with non-optimal overlap. This leads to the appearance of non-proper dissociation behavior at the equilibrium geometry. [36-37]

The problem in treating these, some times severe non-dynamical near-degeneracy problems is for transition metals coupled with the problem to treat the usually strong dynamical correlation problem for the tightly packed electrons in the *d* shell. The main problem in the treatment of non-dynamical correlation effects is that very flexible configuration expansions may be required, while the main problem in the treatment of the dynamical correlation problem is that basis functions with high *l* quantum numbers are in principle required. Transition metal complexes are heavy enough that relativistic effects play an important chemical role. This is particularly true for the third row transition metals, but the relativistic effects cannot be neglected even for the first row transition metals if high accuracy is required. It is this computational challenge to

treat transition metal systems combined with the very large experimental and technical interest that has led to a constantly growing theoretical interest in these systems. [36]

### 3.1.1. Computational treatment of the first row transition metal complexes

Even though the first transition row represents the lightest of the transition metals, molecules containing these metals are usually the most difficult to treat. The large difference in size between the $3d$ and $4s$ orbitals makes computationally tractable. The largest difference in size occurs for nickel, where $\langle 4s \rangle / \langle 3d \rangle$ is as large as 3.36. To the left, this ratio decreases down to 2.03 for scandium. This leads to severe near degeneracy effects when the d bonds are formed since the bonds have to be stretched from the position of optimal overlap. This effect complicates substantially both geometry optimization and the calculation of reliable energies for molecules with elements of this transition raw.

First row transition metal complexes are particularly difficult to handle for several reasons. From standard quantum chemical *Ab initio* view point; there can be a very strong coupling between near degeneracy effects and large dynamical correlation effects for these transition metal complexes. From DFT viewpoint, one difficulty is the strong coupling between correlation effects and exchange effects, at least for cases with unfilled d-shells. These effects are severing for the first raw transition metals. [36, 38]

There are two very important recent developments in the area of electronic structure calculations for transition metal complexes. The first of these concerns the development of DFT methods capable of achieving quantitative accuracy. The second development concerns improvements

in the accuracy of standard chemical methods. For the first transition raw, DFT hybrid methods, give promising results both for geometries and energetics. [39-40]

The particular computational method chosen depends on the desired accuracy (qualitative vs. quantitative), the size of the system, and available computational resources.

## 4. Objective of the project

The general objective of this project is to study molecular properties of transition metal complexes chelated with Schiff base derived from alanine and ninhydrin. The experimentally synthesized complexes are theoretically characterized by different quantum chemical method.

The geometrical structures of the first raw transition metal complexes are investigated and the nature of the ligand, the structural connectivity of the ligand is mainly the goal of this project. The metal complexes are Mn (II), Fe(III), Co(II), Ni(II), and Zn(II). The spectroscopic properties, IR and UV-Vis are computed at different computational methods.

### 4.1. Specific objectives of the project

- Geometry optimization of the ligand and first row transition metal complexes as well as Mulliken charges of the ligand and metal complexes to obtain the minimum energy and most stable geometry before any molecular property calculation is done.
- Computational prediction of IR and UV-Vis properties of the metal complexes and compare with the experimental values
- To determine the ligand binding sites from the IR values and the origins of the electronic spectra of the coordination compounds

## 5. Computational details

The geometry optimization and frequency calculation of the metal complexes were done using the B3LYP functional of the Gaussian 03W [41] program package.

The optimization and frequency calculation of the metal complexes were done using the same basis set. The starting materials of Schiff base, α, L-alanine and ninhydrin, were optimized using B3LYP/6-31G method. The ligand, IDIPA, has been optimized using the same basis set as the starting materials with 6-31G. The optimization and frequency calculation of the metal complexes Mn(II) and Co(II) were done using B3LYP/6-31G method. B3LYP/3-21G(d) method were employed for geometry optimization and frequency calculation of the metal complexes, Fe(III), Co(II) and Ni(II). The Mulliken charges of the ligand and the metal complexes were done.

Electronic spectra of ninhydrin was computed using B3LYP/6-31G, B3LYP/6-31G(d) and ZINDO methods. Electronic spectra of the ligand were calculated using the time dependent B3LYP method with 6-31G basis set as well as using the semiempirical ZINDO method.

The electronic spectra of the metal complexes, Mn(II), Co(II), Ni(II) and Zn(II were calculated at ZINDO level and Fe(III) complex were performed at TD-DFT level using 6-31G(d) basis set. The calculations were performed on a double processor HP Compaq dx 7400 Micro tower, Intel Pentium(R) of version 2002.

# 6. Results and Discussion

For IR vibrational frequency calculation, the B3LYP method with suitable basis set gives reliable data. Hence, the optimization and frequency calculation were done in such a way the results obtained are of course multiplied with a scaling factor of 0.96 which is characteristic vibrational frequency scaling factor of DFT methods (0.9614 for B3LYP/6-31G(d)).

## 6.1. Geometry Optimization

Before calculations of molecular properties of the metal complexes were done, the metal complexes were made to be optimized in the gas phase using B3LYP with standard basis sets.

**Mulliken Charges**: From the calculated Mulliken charges of the atoms in the ligand, the charges on N and O (ketonic) are -0.297 and -0.397. The charge on the hydroxyl O is -0.550 and -0.402 for the carboxylic oxygen. Therefore, the binding sites of the ligand to metal ions are either of these negatively charged ions, (ONOO). Quantitatively, it is possible to figure out the binding sites as –N=C, -O=C- and –O donor atoms to which a coordination will favor. In general, the charge decrease in the metal ions and a negative increase of the donor atoms in the complexes show that the ligand is coordinated to the metal through one of the carbonyl, O, the azomethine N, and the carboxyl O. For example, B3LYP/6-31G optimized structure of Co(II) complex shows reduced Mulliken charge on $Co^{+1.018}$, for the coordinated carbonyl $O^{-0.576,\ -0.496}$ and carboxylic $O^{-0.5,\ -0.547}$ which are higher negative values than the free carbonyl, $O^{-0.361,\ 0.39}$ and carboxyl $O^{-0.429,\ -0.403}$. This is also further supported by the Mulliken charges of the azomethine nitrogen acting as a powerful electron donating with charge $N^{-0.594,\ 0.58}$. Thus, the potential electron donors of the ligand calculated

are therefore a clear indicative of octahedral coordination to the metal complexes.

The optimized structure of the ligand shows bond length of 1.28108 Å for C=N and the ketonic C=O bond lengths are 1.23754 and 1.24538 Å where a coordination takes place.

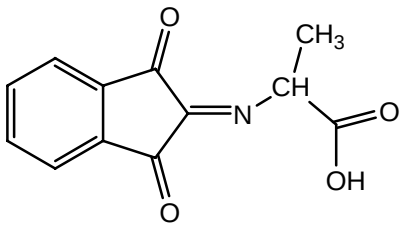


**Fig. II**. Optimized structure of indane-1,3-dione-2-imine-N-2-propoinic acid, IDIPA

The optimized structures for the metal complexes are shown in Fig. III-IV. The optimized structure of Fe(III) complex is consistent with experimental structure in which the Fe-N(1.8813 Å) and the Fe-O (hydroxyl 1.8464 Å) bond lengths, were in good agreement with the octahedral structure of Fe(III) complex.[34] The C=N(1.2931) bond length were larger than the expected C=N double bond in which the bond order is 2. This was generally by the fact that the bond order is decreased due to coordination through N-to the Fe. The coordination were further supported by the elongation of the C=O (1.2785 Å) bond to form a covalent bond with Fe. Although, the strong ionic bond is formed between the basic Fe-O, the Fe-O (1.8464Å) bond length is generally in the same range to the Fe-O (coordinated 1.937Å) in which the former bond length is characteristic of octahedrally bonded ligands in the axial position.

Generally, the $Fe^{3+}$-O bond with high spin $Fe^{3+}$ in octahedral structure is in between 1.84-1.95 Å, characteristic of high spin $Fe^{3+}$ complex in octahedral structure. The Fe-Cl bond length is thus 2.26965Å. [42]

The octahedral structure of Mn(II) in high spin state is the same as the structure of Fe(III) complex in which the number of ligands coordinated to the metal is reduced to one. The same trends are observed for bond lengths of the C=N and C=O. The difference in bond length of the two carbonyls suggests that one of the carbonyl is coordinated to the metal, C=O-1.241 Å (free) and 1.335 Å (coordinated).

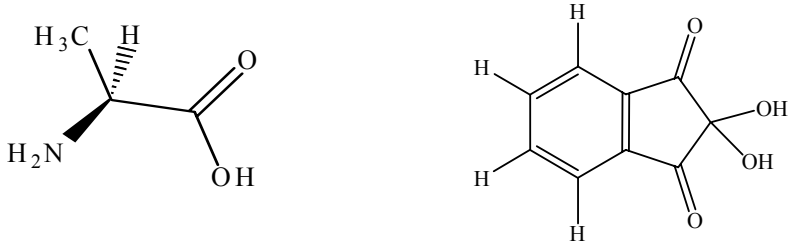


L-Alanine Ninhydrin

**Fig. III.** Optimized Structures of α, L-alanine and Ninhydrin

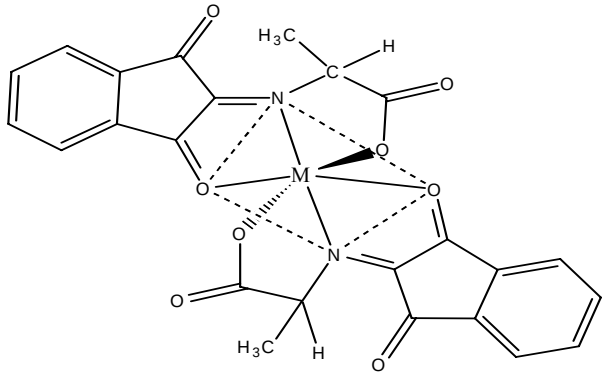


**Fig.IV.** Optimized structures of M = $Co^{2+}$, $Ni^{2+}$, $Zn^{2+}$

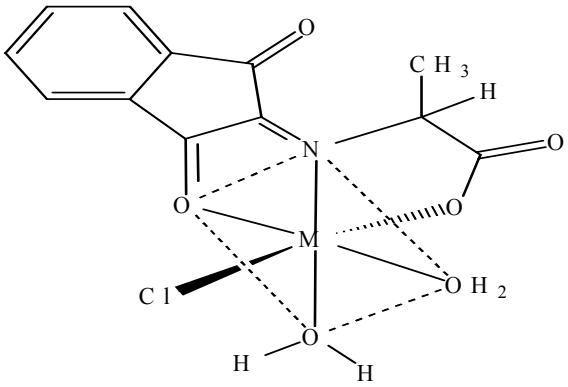


**Fig. V.** Optimized structure M = $Fe^{3+}$

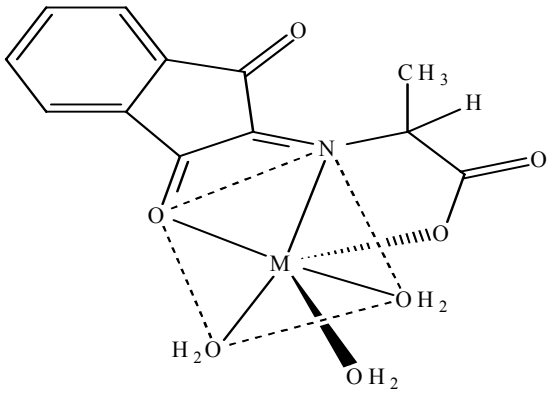


**Fig. VI.** Optimized structure M = Mn(II)

The shift to longer bond length of C=N and C=O in the complexes show that they are involved in coordination with the metal ion. Hence, the ligand is acting as a bidentate through the ON donor atoms. The Fe-O (basic O) with bond length of 1.846 Å is at higher covalency than the Fe-$OH_2$ (1.927 Å). It should be noted that the geometry optimization were done at B3LYP/3-21G(d) theory level and hence the basis set used is relatively small so that the bond lengths deviates from the experiment. The optimized structure of Mn(II) complex shows that the longer bond length of C=O 1.24095 Å (free) to 1.32387 Å suggests that oxygen is covalently bonded to the metal.

The bond length of $Co^{2+}$-O (carbonyl) is 1.93795 Å and C=O is thus 1.30133 Å.

The optimized structure of Zn(II) complex shows a bond length of 1.28563Å for the coordinated C=O which is smaller than the other metal complexes and 1.96352Å for $Zn^{2+}$-N bond length.

After all, the optimized structures show that the minimum energy for the complexes differs from each other. For the cases where satisfactory convergence was obtained the geometries of the complexes remained in a coordination of six, in agreement with the experimental data. [43]

Geometry optimization of the metal complexes using B3LYP level of theory with standard basis sets gives reliable results. The number of ligands coordinated increases from one in Mn(II), Fe(III) to two in Co(II),

Ni(II), Zn(II) metal ions, which is consistent to the size of metal ions to accommodate larger ligands. Despite the fundamental difference among the basis set used for each complex, all calculations suggest a coordination of six to the metal complexes. The ligand is acting as a bidentate through the carbonyl O and the imine N as well as the strongly charged carboxyl O. As a result, the optimized structures were therefore confirming a tridenate monobasic nature of the ligand in such a way a bond lengthen of C=N and C=O bonds to form a covalent bond in all calculation is maintained. From the above structures, one can correlate with the experimentally predicted structure that the optimized geometries are in good agreement with experiment in their octahedral structure. The optimized structures are therefore shown in Fig. III-IV with the number of ligands coordinated differs from each other as, $[Mn(IDIP)(H_2O)_2]^+$, $[Fe(IDIP)H_2OCl]^+$, $M(IDIP)_2$ where M is $Co^{2+}$, $Ni^{2+}$, $Zn^{2+}$.

The octahedral nature of the metal complexes was further supported by the bond angles. In principle, all bond angles within the equatorial plane, within axial plane and between equatorial plane and axial plane are the same, namely, $90^0$. The optimized structure of Co(II) complex is therefore, $\angle O_{ax}$-Co(II)-$O_{ax}$ =$178.2^0$ and $\angle N_{eq}$-Co(II)-$N_{eq}$ = $179.45^0$ , which is comparable to the octahedral structure criteria of $180^0$. The angle between the two nitrogens in the equatorial plane and the oxygen in the axial plane is therefore $85.7^0$ and $93.1^0$. The bond angles for the optimized structure of Ni(II) predicted were in good agreement to the literature values $\angle O_{ax}$-Ni(II)-$O_{ax}$ = $179.47^0$, $\angle N_{eq}$-Ni-$N_{eq}$ = $175.3^0$ and $O_{ax}$-Ni-$O_{eq}$ = $84.8^0$ and $94.08^0$ which deviates from the literature values as it should be $90^0$. The bond angles for the coordinated nitrogen and oxygen in the axial and equatorial, $\angle O_{ax}$-Ni(II)-$N_{eq}$= $83.82^0$ and $96.48^0$. The same trend is observed for the Zn(II) complex.

The optimized structure of Fe(III) complex shows a bond angle of about $170.7^0$ for $\angle O_{ax}$-Fe(III)-$Cl_{ax}$ and $173.2^0$ ($174.2^0$) for $\angle O_{eq}$-Fe(III)-$O_{eq}$ in the equatorial plane. Hence, the presence of the highly electronegative chlorine distorts the octahedral structure of the Fe(III) complex. The optimized structure were also show deviation for the bond angles $\angle O_{eq}$-Fe(III)-$N_{eq}$ = $85.4^0$ and $94.6^0$.

The optimized structure of Mn(II) shows a bond angles comparable to the octahedral bond angles. In perfectly octahedral structure, the axial bonds should make a bond angle of $90^0$ with the equatorial bonds and the $180^0$ with the axial bonds. The bond angles of the axial oxygen with the equatorial bonds are thus, $\angle O_{ax}$-Mn(II)-$O_{ax}$ = $168^0$ and $O_{ax}$-Mn(II)-$O_{eq}$=84, 89, 91, 94.

The optimized structure for $M(IDIP)_2$ (M= $Co^{2+}$, $Ni^{2+}$ and $Zn^{2+}$) show an octahedral structure with small deviation. The computed geometries are therefore in their octahedral structure. For the first two metal complexes Fe(III) and Mn(II), the optimized structure were not perfectly octahedral structure. The bond angles are some what distorted

The optimized structures obtained above were further confirmed that imaginary frequencies for the metal complexes were not found in all calculations. Thus the calculated energies represent a minimum energy and stable geometry.

## 6.2. Infrared spectral studies

The infrared frequencies for the ninhydrin are given in Table 1, the vibrational frequencies are in units of $cm^{-1}$.

**Table**. 1. Infrared spectral characteristics of Ninhydrin [45]

| Comp | B3LYP/6-31G | B3LYP/6-31G(d) | Exper.[34, 44] | Assign. |
|---|---|---|---|---|
| Ninhy | 3445(w) | 3536(s) | 3200-2920(b,s) | ν(OH) |
| | 1694(s), 1665(vs) | 1772 (s) 1744 (s) | 1768,1754, 1720(s) | ν(C=O) |
| | 1585(m) | 1585(m) | 1590(s) | ν(C=C)aro |
| | 3109(w), 3092(w) | 3099 (s), 3084 | - | ν(=C-H) arom |
| | 727(m) | 721(s) | - | δ(=C-H) in plane |
| | 466(m), 395(s) | 418(s) | - | δ(O-H) |

vs – very strong; s - strong; m – medium; w - weak

Calculations of the vibrational frequencies of ninhydrin using the B3LYP level of theory (scaled with 0.9614) are in good agreement with the experiment.

A very strong absorption at 3536 $cm^{-1}$ is attributed to the O-H stretch. The O-H stretching absorption of the hydroxyl group is very sensitive to hydrogen bonding. In the gas phase, O-H stretch exhibits a sharp absorption in the range 3560-3650$cm^{-1}$. Thus the large differences between experiment and the calculated values at B3LYP/6-31G(d) and B3LYP/6-31G indicates that the OH is free of H-bonding.

The 1, 3 dicarbonyl functionality behavior of the ninhydrin is therefore supported by the two calculations in which the B3LYP/6-31G(d ) method is fairly in good agreement with experimental ones. In both calculation, a third C=O stretch is not observed, hence the third C=O stretch is due to the intermediate obtained when the ninhydrin is in solution and made to condense. Hence, the calculation in both cases is therefore carried out in the gas phase which doesn't support a third C=O absorption, 1768 $cm^{-1}$.

The significant IR bands for the ligand as well as for its metal complexes and their assignments are compiled and represented in Table 2.

**Table 2.** Infrared spectral data of the metal complexes of IDIPA calculated with B3LYP using different basis sets (IR frequencies are given $cm^{-1}$) [34, 44]

| Compound | α,L-ala[b] | Ligand[b] | Mn(II)[b] | Fe(III)[a] | Co(II)[b] | Ni(II)[a] | Zn(II)[a] |
|---|---|---|---|---|---|---|---|
| ν(OH) (ν($NH_2$)) | 3543(w) (3441w, 3353w) | 3535(w) | 3695(m)-3511(w) | 3521 (s) 3466 (s) 3390 (m), 3314(m) | - - | - | - |
| ν(C=O) | - | 1760(m) 1735(s) | 1670(m) | 1695 (s) | 1664(m) 1643(vs) | 1686(m) 1663(vs) | 1696(s) 1655(vs) 1646(w) |
| $\nu(C=C)_{arom}$ | - | 1605(w) | 1568(w) | 1540 (s) | 1587(w) | 1545(w) | 1576(w) |
| $\nu_a$(COO | 1770(vs | 1780(vs) | 1690(vs) | 1720(vs) | 1645(vs) | 1697(vs) | 1687(vs) |
| ν(C=N) | - | 1640(w) | 1502(vs) | 1582 (vs) | 1556(vs) | 1581(s) | 1596(vs) |
| δ(CH, $CH_3$ | 1318(w) 1465(w), 1387(w) | 1283(w) 1411(w) | 1291(w) 1391(s) | 1346. (m), 1398 (1489.) | 1335(vs) 1463(m) | 1315(vs) 1416(vs) | 1418(w) 1498(w) |

[a]3-21G(d) [b]6-31G , ν- stretching; out of plane bending; δ- bendingvs – very strong; s - strong; m – medium; w - weak

Although the comparison of IR frequencies is not possible between the metals, the results obtained at smaller basis set are not far from the experimental ones. The IR spectrum of α, L-alanine exhibits $\nu_{NH2}$ at 3441cm$^{-1}$ and 3353 cm$^{-1}$ is not observed in the metal complexes. The higher frequency is associated with the asymmetric stretching characteristic of N-H and the lower frequency is also due to the symmetric stretching of N-H. The O-H stretch is observed for the compounds ninhydrin, α, L-alanine and two of the metal complexes, Fe(III) and Mn(II). The free O-H stretch in the metals is due to the presence of coordinated water to the metals thus reducing the number of ligands coordinated to the metal. The solvent is therefore replacing the ligand, which is greatly supported by the lower frequencies characteristic of O-H bending. Thus, the number of ligands coordinated to the metal is greatly influenced by the metal size.

A clear indication of coordination of the ligand through one of the carbonyls is observed for the C=O stretch. Generally, the C=O stretch is 1650-1780 cm$^{-1}$. The C=O stretch in the metal complexes is generally lower than the experimental values. For Fe(III) complex, the C=O stretch deviates from the experimental values by +10-15 cm$^{-1}$. Hence, the frequency calculation using B3LYP/3-21G(d) for the C=O stretch is therefore in good agreement with the experimental.

The vibrational frequencies for Mn(II) complex obtained at the DFT level of B3LYP/6-31G greatly deviate from the experimental. The Vibrational frequency of C=O (coordinated) in the Mn(II) complex is 1561 and 1670 cm$^{-1}$ for free C=O bond. The lower vibrational frequencies for the C=O stretch at 1561 cm$^{-1}$ is therefore the strong coordination to metal ions. The results are in good agreement to the experiment, 50-90 cm$^{-1}$. The infrared frequencies for the carbonyl groups in the ligand are shifted from 1735(s) to 1660 cm$^{-1}$ and 1781 cm$^{-1}$ to 1689 cm$^{-1}$. The shift to lower frequencies indicates the involvement of one of the two carbonyl groups

of the ligand in coordination with the metal ion. The coordination of one of the carbonyl to the metal ion is also well behaved by the C=O stretch at 1561 $cm^{-1}$. Thus, the predicted frequencies for C=O in the complex at the B3LYP/6-31G are generally well defined and gives reliable results comparable to the experiment.

Infrared frequencies of the Fe(III) complex computed at the B3LYP/3-21G(d) are given in table 2.

The presence of $\nu_{O-H}$ stretch at 3521-3314 $cm^{-1}$ indicates the coordination of water molecules to the metal ion and further confirmed by the O-H bending observed in the spectrum from 435-575$cm^{-1}$. Moreover, the presence of coordinated water to the Mn(II) and Fe(III) complexes is supported by other bands in the region 1520-1550 $cm^{-1}$. The lower shift of the C=O frequencies for the metal ion reflects the accuracy of the 3-21G(d) basis set for an octahedrally coordinated Fe(III) complex in high spin state. The C=O stretch in this complex are 10-15 $cm^{-1}$ larger than the experiment.

The IR frequencies for the Ni(II) complex computed using 3-21G(d) basis set were generally in good agreement with the experiment for the carbonyl vibrational frequencies (35 $cm^{-1}$ lower) and the vibrational frequency of azomethine group (C=N) is about 65 $cm^{-1}$ discrepancy from the experiment. The lower values for the carbonyl indicates that the C=O bond is well coordinated to the metal and therefore the basis set employed is however well to reproduce the metal-ligand strong coordination. In more general, even though the smaller 3-21G(d) basis set is employed for Ni(II) complex, can reproduce relatively reliable result consistent to the experiment .

As a result, the infrared spectra computed for the Ni(II) complex is clearly indicating the same trend as the other basis sets that the vibrational frequency of the azomethine and carbonyl in the ligand shifts

to lower frequency in the metal complexes. The IR frequencies of C=O and azomethine groups in Zn(II) complex appear in between 1696-1655 $cm^{-1}$ and 1596 $cm^{-1}$ of appreciable difference with the experiment of 37-55 $cm^{-1}$ and 88 $cm^{-1}$, respectively.

In all computation, the vibrational frequencies are generally in good agreement with the experimental results that the relative error is in the range 2-7%. The vibrational frequencies obtained computationally are generally with a relative error of 10%. [3]

In all computation, the vibrational frequencies are generally higher than the experimental values with small discrepancy and therefore be employed for molecular properties of the transition metal complexes. It is important to note that the hybrid B3LYP method is a reliable method in reproducing IR frequencies of the first row transition metal complexes in a more low computational cost. The method can variably used with different standard basis set for IR prediction.

The IR frequencies for the aromatic C=C stretch in the metal complexes are generally lower than the ligand and differ by 10-48 $cm^{-1}$ from the experiment besides the basis set employed for each metal complexes are different. The presences of medium bands at 745-760 $cm^{-1}$ in the metal complexes are due to ortho- di- substituted aromatic ring in the ligand and the results are consistent with experiment of 10-15 $cm^{-1}$ error.

The IR frequency for $\nu_{C=N}$ of the ligand and the metal complexes is a very interesting feature of the metal complexes through which a coordination with the metal ions is at most favored. The results obtained for $\nu_{C=N}$ of the ligand calculated at B3LYP/6-31G theory level is thus 1640 $cm^{-1}$. Generally, the usual frequency at which azomethine group (C=N) appears is in the range 1600-1670 $cm^{-1}$. The calculated value is therefore consistent with the literature values. In the metal complexes, this absorption appears to lower frequencies. Its negative shift of about 50-90

$cm^{-1}$ is a clear indication of the participation of the azomethine nitrogen in coordination. However, the calculated values are generally higher than the experimental values about 85 $cm^{-1}$. The IR frequency of the azomethine of the Mn(II) complex calculated using B3LYP/6-31G is 1503 $cm^{-1}$ ($2cm^{-1}$) in good agreement with the reference value. A similar situation is observed in the case of Co(II) complex with 44 $cm^{-1}$ larger from the reference value and therefore in a reasonable agreement. The absorption bands of $\nu_{C=N}$ in the metal complexes, Fe(III), Ni(II) and Zn(II) are fairly higher of about 85 $cm^{-1}$. Therefore, the B3LYP/6-31G method predicts the $\nu_{C=N}$ infrared frequency consistent to the experiment. The calculated IR frequencies for the azomethine group in the metal complexes show that the C=N- group is coordinated to the metal through the nitrogen donor atom.

The structure and IR frequency difference of metal complexes are greatly influenced by the metal –ligand interaction and thus become the specific and most important way to differentiate these complexes from each other based on their chemical nature and size of the metal. Thus, from the geometry optimization, it was possible to differentiate the metal-ligand bond length of the complexes and therefore the same trend is generally obtained for the metal –ligand IR frequencies.

The metal- ligand bands observed for the metal complexes were at lower frequencies in the range 242-780 $cm^{-1}$ characteristic of the M-N, M-O bonds. A very interesting band at 242 $cm^{-1}$ were only observed for Fe(III) complex and suggests that Fe(III) is bonded to halogen atom Cl different from other complexes. The absorption band for M-N and M-O appear only for the metal complexes.

The C-O stretch is generally in the range 1000-1300 $cm^{-1}$. The negative shift of the C-O stretch is therefore a clear indication of coordination of the oxygen with metal ions. This coordination is further confirmed by the presence of bands for M-O bond. However, the results were deviating

from the experimental values (140cm$^{-1}$ lower). The absorption band at 707 cm$^{-1}$ (20 cm$^{-1}$ larger) and 638 cm$^{-1}$(32 cm$^{-1}$) are assigned to $Zn^{2+}$-N and $Zn^{2+}$-O bands and lower frequency bands were also observed at 599 and 547 cm$^{-1}$. Mn(II) complex show $Mn^{2+}$-N and $Mn^{2+}$-O bands at 707 and 638 cm$^{-1}$, respectively. The IR spectra of Fe(II) and Mn(II) show HOH bending at 523 cm$^{-1}$ and 574 cm$^{-1}$, respectively. Hence, the HOH bending were not observed in the IR spectra of the three metal complexes, Co(II), Ni(II) and Zn(II). The coordination of the carboxylic oxygen of the ligand to metal ions was determined from the IR spectrum of metal complexes computed theoretically. Despite the difference in the basis set for metal complexes, the B3LYP method reproduces reasonable IR frequency of the metal-ligand in good agreement with the experiment.

Finally, it could be concluded that IDIPA behaves as a tridentate ONO donor involving a carbonyl oxygen, a carboxyl oxygen and an azomethine oxygen in coordination.

## 6.3. Electronic Spectral Studies

All metal complexes show electronic transitions characteristic of the ligands. The presence of non-bonded electrons and π electrons in the ligand attributes to different electronic transitions. The electronic spectral data for ninhydrin calculated with time dependent-density functional theory, TD-DFT(B3LYP) method using two basis set is shown in Table 3.

**Table 3**. Electronic spectral data of Ninhydrin (three Excitations)

| Stat | ZINDO/S | | | TD-DFT/6-31G | | | TD-DFT/6-31G(d) | | |
|---|---|---|---|---|---|---|---|---|---|
| e | E | λ | *f* | E | λ | *f* | E | λ | *f* |
| 1 | 4.36 | 284 | 33.5 | 3.38 | 367 | 0. 2 | 3.28 | 378 | 0. 2 |
| 2 | 5.42 | 229 | 912.9 | 3.43 | 361 | 1.7 | 3.65 | 340 | 0. 9 |
| 3 | 5.63 | 220 | 395.0 | 4.3 | 288 | 0. 4 | 4.23 | 294 | 0. 7 |

E/eV; λ/nm; $f$x10$^{-3}$

The electronic spectra of ninhydrin show that transitions are formally weak band in which the absorption intensity tends to be much lower and are commonly assigned to two transitions which are characteristic of carbonyl and benzene electronic transitions. The transitions for the ninhydrin using TD-DFT were done for the first 3 states. However, for ZINDO method, electronic transitions were done for the first 40 states and therefore the more intense (large *f*) were taken for comparison

From TD-DFT calculation, bands at longer wavelength 370 nm are characteristic of the $n \rightarrow \pi^*$ transitions of carbonyl group and the lower 288-294 nm is assigned to the $\pi \rightarrow \pi^*$ transitions of benzene moiety. As we increase the possible excitation states, it is possible to observe all electronic excitations. [34, 44]

Over all 40 excited states of ZINDO/S calculation, the lower wavelength indicates that electronic excitations are allowed excitations in which the value of oscillator strength is higher for those allowed transitions. However, the oscillator strength is therefore the bridge between, since for more allowed transitions *f* gets larger. Hence, excitation state 2 is a characteristic of $\pi \rightarrow \pi^*$ transition. Generally, both DFT and ZINDO methods give electronic spectral data of complementary values of the transition and fairly correlate with the experimental ones. All complexes were therefore calculated at the ZINDO/S level beside that its accuracy is fairly comparable with the TD-B3LYP in which the computational cost is thus high. The electronic spectral data for metal complexes calculated using ZINDO/S method are given in table 5.

**Table 4**. Electronic spectral data of ligand calculated at the ZINDO method and TD-B3LYP with 6-31G basis set

| Excit. | ZINDO | | | TD-DFT/6-31G | | |
|---|---|---|---|---|---|---|
| | E/eV | λ/nm | *f* | E/eV | λ/nm | *f* |
| 1 | 4.37 | 284 | 0.1757 | 4.09 | 303 | 0.0313 |
| 2 | 4.78 | 259 | 0.743 | 4.82<br>4.87 | 257<br>254 | 0.1735<br>0.3748 |
| 3 | 5.65 | 219 | 0.3998 | 5.58<br>5.68 | 230<br>218 | 0.1357<br>0.128 |

The ZINDO method is therefore relatively reliable method as good as the TD-DFT method; where TD-DFT is regarded today as the more accurate computational method [46], but given the high computational costs involved, especially with larger molecules. The two calculations show that the transitions observed in the region 33,112 $cm^{-1}$-35, 200 $cm^{-1}$ (284-315 nm) is assigned to the n→π * transitions of the carbonyl group with 300-1000 $cm^{-1}$ lower than the experiment. A weak intensity and therefore characteristic band of the azomethine is assigned to n→π transition observed at 23,924 $cm^{-1}$.

After all, the strong and high-energy electronic transitions were predicted to be π →π * transitions of benzene moiety in the region 38,910-43,660 $cm^{-1}$. Hence, the ZINDO method is thus comparable accuracy to TD-DFT method. ZINDO method is commonly used to analyze the electronic structure and spectra of transition metal complexes. [46]

The electronic spectral data of metal complexes are given below in table 5

**Table 5**. Electronic spectral data of metal complexes of IDIP and their assignments obtained at ZINDO/S method

| Complex | Non-ligand electronic Spectral bands (in $cm^{-1}$) | | Assignment [34] |
|---|---|---|---|
| | Calc. | Exper.[34] | |
| Mn(II) | 27,202, 24,938 | 27, 397 | $^6T_{1g} \rightarrow {}^4T_{2g}(D)$ and $^6A_{1g} \rightarrow {}^6A_{1g}(G)$ |
| | 31,960, 33,830 (36,539) | 31,250, 35, 587 | Mixed bands of $^6A_{1g} \rightarrow {}^4E_g(D)$, $^6A_{1g} \rightarrow {}^4T_{1g}(P)$ |
| Fe(III)[a] | 26, 530<br>26,220-25,680<br>13, 827 | 28571<br>27397<br>12, 739 | $^6A_{1g} \rightarrow {}^4E_g(G)$, $^6A_{1g} \rightarrow {}^4A_{1g}$<br>$^6A_{1g} \rightarrow {}^4E_g(D)$, $^6A_{1g} \rightarrow {}^4T_{1g}(D)$<br>$^6A_{1g} \rightarrow {}^4T_{2g}(G)$ and $^6A_{1g} \rightarrow {}^4T_{1g}(G)$ |
| Co(II) | 28, 530<br>16, 522,<br>14, 694 | 31, 250*<br>14, 837 | CT<br>$^4T_{1g} \rightarrow {}^4A_{2g}$ and $^4T_{1g} \rightarrow {}^4T_{1g}(P)$ |
| | 13, 432,<br>11, 657 | 12,690 - 12,547 | $^4T_{1g} \rightarrow {}^4T_{2g}$ |
| Ni(II) | 10, 225<br>14, 165<br>26,334-27,447<br>17, 704 | 10, 460<br>15,385<br>27,174<br>1660* | $^3A_{2g} \rightarrow {}^3T_{2g}$<br>$^3A_{2g} \rightarrow {}^3T_{1g}$<br>$^3A_{2g} \rightarrow {}^3T_{1g}(P)$<br>$^3A_{2g} \rightarrow {}^1T_{1g}$ |
| Zn(II) | - | | - |

[a]TD-DFT/6-31G(d); * [44]

From the above table 5, the electronic transitions of metal complexes calculated at ZINDO level are fairly in good agreement to the experiment. The Fe(III), Mn(II) complexes have a $d^5$ configuration and hence the energy levels for $d^5$ ion and its equivalent hole are the same. Thus, complexes of these ions are faintly colored. The ground sate of high spin octahedrally coordinated $Mn^{2+}$ and $Fe^{3+}$ complexes is therefore $^6A_{1g}$ in which the ground state term symbol of the metal complexes is $^6S$ and other terms $^4G$, $^4P$, $^4F$, $^4D$ next to the ground state term symbol. There are no other terms of sextet spin multiplicity and hence the transitions calculated are generally mixed and weak intensity of the characteristic

forbidden d-d transitions. However, very weak spin forbidden transitions to quartet were calculated in the metal complexes. Mn(II) and Fe(III) complexes are therefore in their high spin sate in which the metal-ligand interaction is highly covalent in nature**.**

The ground state term symbol Co(II) in the presence of ligand in octahedral structure is $^4F$ and hence the ground state is thus with $^4T_{1g}$ symmetry. Three spin allowed ligand field absorption bands were calculated and they are in good agreement to the experiment. These absorption bands are therefore characteristic of an octahedral geometry of Co(II) complex in high spin sate.

The $d^8$ metal complex of Ni(II) in its octahedral structure show three electronic transitions which are allowed transitions by spin multiplicity selection rules. The ground state term symbol is $^3F$ and in the presence of ligand field the ground state term is thus $^3A_{2g}$ in octahedral coordination. The transitions observed were therefore characteristic of the Ni(II) complex in octahedral coordination.

The Zn(II) complex has therefore a $d^{10}$ configuration and its diamagnetic nature of the metal fails to absorb in the visible region.

The metal complexes show ligand characteristic bands of generally 38,000$cm^{-1}$ which are characteristic of $\pi \rightarrow \pi^*$ as well as some of the electronic transitions of the metal complexes were also obscured by the bands from the ligand in the region of 20,000-26,000 $cm^{-1}$ assigned to the $n \rightarrow \pi^*$ transitions characteristic of the azomethine and carbonyl groups. Therefore, the electronic spectral calculations show that the metal complexes are in their octahedral coordination that the ligand – metal interaction resulting in a large electron delocalization and hence good covalent character of the metal ligand character. The covalent character is high in the $d^5$ metal complexes (Mn(II), Fe(III)) and increases from Co(II) to Ni(II) complexes.

## 7. Conclusion

The computational prediction of infrared spectral property of metal complexes, Mn(II), Fe(III), Co(II), Ni(II) and Zn(II) coordinated to the ligand IDIPA, water and Cl using B3LYP with 6-31G, 3-21G(d), 6-31G, 3-21G(d) and 3-21G(d), respectively, show good agreement with the experiment in spite of using different basis sets for each complex. The hybrid DFT method, B3LYP is therefore a very good method to study molecular properties of transition metal complexes.

Electronic spectral calculations of transition metal complexes using ZINDO are in a reasonable agreement with the experimental values. The ligand, IDIPA, is an intermediate Schiff base derived from α, L-alanine and ninhydrin is tridentate monobasic potential ligand with ONO donor atoms for the first row transition metal complexes in their octahedral structure. The theoretical calculations are illustrating the experimental ones that the ligand IDIPA is the potential ligand, behaves as a tridentate ONO donor involving an azomethine nitrogen, carbonyl oxygen and the carboxyl oxygen in coordination. The theoretical calculations are thus supporting an octahedral structure of the metal complexes in which the coordination is six in consistent to the experiment. However, the octahedral nature of the first two metal complexes Fe(III) and Mn(II) is distorted as compared with perfect octahedral structure.

Although much works are needed to compute molecular structure of the transition metal complexes, B3LYP with standard basis set are fairly enough to calculate structure and the infrared spectra of the metal complexes and semiempirical ZINDO method is a good model reproducing very well electronic spectra of the metal complexes as comparable to the experiment where higher computational methods are very cost enough.

## References


[1] Levine, I.N., *Quantum Chemistry,* 5th Ed., Prentice –Hall, Inc., New Jersey, 2000.

[2] Young, D.C., *Computational Chemistry: A Practical Guide for Applying Techniques to Real-World Problems*, John Wiley & Sons, New York, 2001.

[3] Foresman, J.B., and Frisch, Æ., *Exploring Chemistry with Electronic Structure Methods,* 2nd Ed., Gaussian Inc., Pittsburgh, PA, 1996.

[4] Cramer, C.J., *Essentials of Computational chemistry: Theories and Models*, 2nd Ed., John Wiley & Sons, Chichester, 2004.

[5] Jenn-Huei, L. and Allinger, N.L., *J. Am. Chem. Soc.*, 1989, **111**, 8576.

[6] Rappie, A.K.; Casewit, C.J.; Colwell, K.S.; Goddard III, W.A.; and Skiff, W.M., *J. Am. Chem. Soc.,* 1992, **114**, 10024.

[7] Jensen, F., *Introduction to Computational Chemistry*, John Wiley & Sons, Chichester, 1999.

[8] Clementi, E. and Coronogiv, G., *Int. J. Quan. Chem.*, 1997, **62**, 571.

[9] Bartlett, R.J., *J. Phys. Chem.*, 1989, **93**, 1697.

[10] Bartlett, R.J., *Ann. Rev. Phys. Chem.,* 1981, **32**, 358.

[11] Krishnan, R. and Pople, J.A., *Int. J. Quan. Chem.,* 1978, **14**, 91.

[12] Hohenberg, P. and Kohn, W., *Phys. Rev. B*, 1964, **136**, 864.

[13] Kohn, W. and Sham, L. J., *Phys. Rev. A*, 1965, **140**, 1133.

[14] Vosko, S.J.; Wilk, L.; and Nusair, M., *Can. J. Phys.*, 1980, **58**, 1200.

[15] Perdew, J.P., and Wang, Y., *Phys. Rev. B*, 1986, **33**, 8800.

[16] Becke, A.D., and Roussel, M.R., *Phys. Rev. B*, 1988, **38**, 3098.

[17] Lee, C., Yang, W. and Parr, R.G., *Phys. Rev. B*, 1988, **37**, 785.

[18] Koch, W. and Holthausen, M.C., *A Chemist's Guide to Density Function Theory*, 2nd Ed., John Wily & Sons, Wienheim, 2000.

[19] Parr,R. G. and Yang, W., *Density-Functional Theory of Atoms and Molecules*, Oxford University Press, New York, 1989.

[20] Frisch, A. and Frisch, M.J., *Gaussian 98 User's Reference*, Gaussian Inc., Pittsburgh, PA, 1998.

[21] Habibollahzadeh, D.; Grodzicki, M.; Seminario, J.M.; and Politzer, P., *J. Phys. Chem.,* 1991, **95**, 7699.

[22] Kotochigova, S.; cJulienne, P.S.; and Tiesinga, E., *Phys. Rev. A*, 2003, **68**, 22501.

[23] Hessel, M.M.; Smith, E.W.; and Drullinger, R.E., *Phys. Rev. Lett.*, 1974, **33**, 1251.

[24] Amos, R.D.; Gaw, J. F.; and Handy, N.C., *J. Chem. Soc.*, *Faraday Trans.* 2, 1988, **84**, 1247.

[25] Scott, A.P. and Radom, L., *J. Phys. Chem.*, 1996, **100**, 16502.

[26] Baker, J.; Jarzecki, A.A.; and Pulay, P., *J. Phys. Chem. A*, 1998, **102**, 42.

[27] Pavia, D.L.; Lampman, G. M.; and Kriz, G.S., *Introduction to Spectroscopy*, 3rd Ed., Thomson Learning, Inc., Australia, 2001.

[28] Haris, D.C. and Bertolucci, M.D, *Symmetry and Spectroscopy*: *An Introduction and Eelectronic Spectroscopy*, Dover Publication, Inc., New York, 1989.

[29] Barltrop, J.A. and Coyle, J.D., *Excited State in Organic Chemistry*, John Wiley & Sons, NewYork, 1975.

[30] Sathyanarayana, D.N., *Electronic Absorption Spectroscopy and Related Techniques*, Orient BlackSwan, India, 2001.

[31] Gerloch, M. and Constable, E. C., *Transition Metal Chemistry*, Jon Wiley & Sons, Weinheim, 1994.

[32] Huheey , J.E.; Kieter, E.A.; and Kieter, R.L., *Inorganic Chemistry,* Harper Collins, New York, 1993.

[33] Cotton, R.A. and Wilkinson, G., *Advanced Inorganic Chemistry,* 5th Ed., John Wiley & Sons, New York, 1989.

[34] Getahun, M.D.; Raju, V.J.T.; and Retta, N., *Bull. Chem. Soc. Ethiop.*, 2002, **16**, 53.

[35] Temel, H. and İlhan, S., *Russ. J. Coord. Chem.*, 2007, **33**, 918.

[36] Siegbahn, P.E.M., *Advances in Chemical Physics*, Volume XCIII, John Wiley & Sons, 1996.

[37] Darkhovskii, M.B.; Soudackov, A.V.; and Tchougr´eeff, A.L., *Theor. Chem. Acc.*, 2005, **114**, 97.

[38] Siegbahn, P.E.M. and Blomberg, M.R.A., *Theor. Chem. Acc.*, 1997, **97**, 72.

[39] Atanasov, M.; Comba, P.; Martin, B.; et al., *J. Comput. Chem.* 2006, **27**, 1263.

[40] Siegbahn, P.E.M. and Blomberg, M.R.A. *Chem. Rev.* 2000, **100**, 421.

[41] Frisch, M. J.; Trucks, G. W.; Schlegel, H. B.; Scuseria, G. E.; Robb,M. A.; Cheese, J.R.; Iyengar, S.S.; Tomasi, J.; Barone, V.;Mennucci, B.; Cossi, M.; Scalmani, G.; Regga, N.; Peterson, G.A.; Nakatsuji, H.; Hada, M.; Ehara, M.; Toyota, K.; Fukuda R.; Hasegawa, J.; Ishida, M.; Nakajima, T.; Honda, Y.; Kitao, O.; Nakai, H.; Klene, M.; Li, X.; Knox, J. E.; Hratchian, H. P.; Cross, J. B.; Bakken, V.; Adamo, C.; Jaramilo, J.; Gomp+erts, R.; Stratmann, R. E.; Yazyev, O.; Austin, A. J.; Cammi, R.; Pomelli, C.; Ochterski, J. W.; Ayala, P. Y.; Morokuma, K.; Voth, G. A.; Salvador, P.; Dannenberg, J. J.; Zakrzewski, V. G.; Dapprich, S.; Daniels, A. D.; Strain, M. C.; Farkas, O.; Malick, D. K.; Rabuck, A. D.; Raghavachari, K.; Foresman, J. B.; Ortiz, J. V.; Cui, Q.; Baboul, A. G.; Clifford, S.; Cioslowski, J.; Stefanov, B. B.; Liu, G.; Liashenko, A.; Piskorz, P.; Komaromi, I.; Martin, R. L.; Fox, D. J.; Keith, T.; Al-Laham, M. A.; Peng, C. Y.; Nanayakkara, A.; Challacombe, M.; Gill, P. M. W.; Johnson, B.; Chen, W.; Wong, M. W.; Gonzalez, C.; and Pople, J. A., *Gaussian 03, Revision E.01,* Gaussian, Inc., Wallingford CT, 2004.

[42] McNeill, E.A. and Scholer, F.R., *J. Am. Chem. Soc.,* 1977, **99**, 6242.

[43] Rochon, F.D.; Melanson, R.; and Farrel, N., *Acta. Crystallogr. Sec. C.*,

1993, **49**, 1703.

[44] Rao, N.S.R.R.M.M.K. and Reddy, M.G.R., *Biol. Met.*, 1990, **3**, 19.

[45] Sadtler Research Laboratories Inc., 1996 *Standard Spectra*, #21078K.

[46] Lever, A.B.P, and Gorelsky, S.I, *J. Organomet. Chem.,* 2001, **635**, 187.